

Conclusion

By combining innovative material engineering with advanced synchrotron analysis at the NSRRC, the team has demonstrated a BEOL-compatible SOT-MRAM solution that overcomes a major roadblock for commercial semiconductor integration. This work underscores the vital role of nanodiffraction techniques in characterizing next-generation spintronic materials. (Reported by Yen-Lin Huang, National Yang Ming Chiao Tung University)

This report features the work of Yen-Lin Huang and his collaborators published in Nat. Electron. 8, 794 (2025).

TPS 21A X-ray Nanodiffraction

- n-XRD, ED-XND
- Materials Science, Electronic Device, Microstructural Domain Image

References

1. H.-S. P. Wong, S. Salahuddin, Nat. Nanotechnol. **10**, 191 (2015).
2. C.-F. Pai, L. Liu, Y. Li, H. W. Tseng, D. C. Ralph, R. A. Buhrman, Appl. Phys. Lett. **101**, 122404 (2012).
3. Y.-L. Huang, M. Song, C.-M. Lee, Y.-W. Chen, C.-Y. Chiang, S.-H. Chou, L.-C. Hsu, H.-J. Liu, G.-L. Chen, S.-Y. Yang, Y.-J. Chang, I.-J. Wang, Y.-C. Hsin, Y.-H. Su, J.-H. Wei, F. Xue, S. X. Wang, X. Bao, Nat. Electron. **8**, 794 (2025).

Highly Crystalline Selenium-Substituted Acceptor-Donor-Acceptor-Type Acceptor Enabling High-Mobility N-Type Transistors

Selenium-substituted non-fullerene acceptor CB-2Se exhibits a single-crystal-like thin-film packing after thermal annealing, resulting in exceptional n-type organic field-effect transistor mobility of $1.18 \text{ cm}^2 \text{ V}^{-1} \text{ s}^{-1}$ with excellent air stability.

In 2019, the non-fullerene acceptor (NFA) material Y6 emerged as a groundbreaking development in organic solar cells, achieving a power conversion efficiency of 15.7%.¹ This milestone significantly advanced the development of organic photovoltaic (OPV) materials. Y6 features an A-D_NA'_ND-A-type molecular architecture with a characteristic C-shaped geometry, incorporating an electron-deficient thiodiazole (Tz, A' unit) into the core. This structural motif effectively modulates intermolecular interactions and molecular packing. Recently, a structurally simplified A-D_NB_ND-A NFA, CB16, was developed, employing an unsubstituted *ortho*-benzodipyrrole (*o*-BDP) core derived from Y6 by removing the A' moiety.² Both CB16 and Y6 derivatives share a key structural feature: the *o*-BDP core. This semi-circular, π -conjugated unit facilitates the formation of three-dimensional interpenetrated networks through self-assembly, promoting multidirectional charge transport pathways. As a result, inverted OPVs based on CB16 achieved efficiencies comparable to those of Y-series materials. Ongoing structural refinement of CB-based architectures is expected to drive the advancement of next-generation acceptor-donor-acceptor-type (A-D-A-type) NFAs.

Despite the rapid progress of OPV technologies, NFAs have yet to demonstrate high electron mobility in organic field-effect transistors (OFETs). To date, the development of n-type OFETs remains limited, particularly for solution-processable systems under ambient conditions. Key challenges include the suboptimal molecular ordering and stacking behavior of NFAs, which restrict their charge-transport capabilities. Reports of n-type OFETs with electron mobilities exceeding $1 \text{ cm}^2 \text{ V}^{-1} \text{ s}^{-1}$ remain scarce, and such performance is typically observed only in single-crystal devices—systems that are difficult to fabricate and scale, thus limiting their practical applicability. Therefore, there is an urgent need to design new NFAs that can self-assemble into highly crystalline, single-crystal-like domains in thin films *via* solution processing. However, rational design strategies for such materials remain underdeveloped. Notably, C-shaped NFAs based on the *o*-BDP core exhibit extensive π - π interactions in the solid state, enabling the formation of interpenetrating three-dimensional networks. These networks provide diverse charge transport pathways, underscoring their potential for single-component OFET applications.

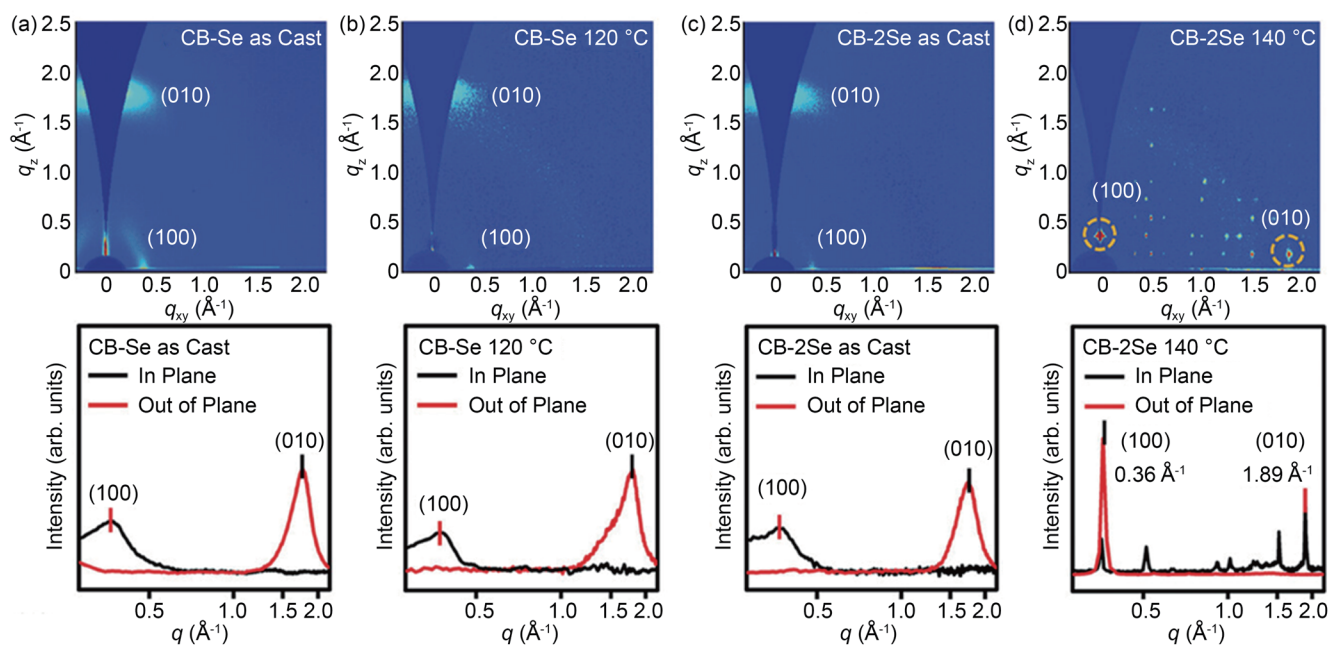


Fig. 1: Two-dimensional GIWAXS patterns of (a) as-cast CB-Se and (b) CB-Se neat film thermally annealed at 120 °C for 10 min; (c) as-cast CB-2Se and (d) CB-2Se neat film thermally annealed at 140 °C for 10 min, showing the appearance of highly oriented diffraction peaks. [Reproduced from Ref. 3]

Recently, Yen-Ju Cheng's team (National Yang Ming Chiao Tung University) implemented a selenium-substitution (Se-substitution) strategy on the central D_NB_ND ladder- π -core, yielding asymmetric CB-Se and symmetric CB-2Se. Due to the higher polarizability of Se atoms, introducing a selenophene unit into organic semiconductors has proven to be an effective strategy for strengthening intermolecular Se-Se or Se- π interactions. These features enhance the crystallinity of the NFAs and promote the formation of single-crystal molecular assemblies, thereby enabling excellent ambipolar OFET performance. Notably, the symmetric CB-2Se exhibited an outstanding electron mobility of $1.18 \text{ cm}^2 \text{ V}^{-1} \text{ s}^{-1}$ and a hole mobility of $0.63 \text{ cm}^2 \text{ V}^{-1} \text{ s}^{-1}$ in the OFET device, along with exceptional air stability.

To elucidate the molecular packing and film morphology of the two NFAs, grazing-incidence wide-angle X-ray scattering (GIWAXS) measurements were conducted at **TPS 25A (Fig. 1)** with experimental assistance from Yi-Wei Tsai, Jih-Ming Lin, and U-Ser Jeng from the NSRRC. The as-cast neat films of CB-Se and CB-2Se exhibited pronounced (010) diffraction peaks in the out-of-plane direction and broad (100) reflections in the in-plane direction, indicative of a predominantly face-on orientation. When both NFAs were subjected to thermal annealing for 10 min, CB-Se still showed a face-on orientation. However, the initially arc-like diffraction pattern of the as-cast CB-2Se film was converted into a discrete point-like pattern, indicating the formation of highly crystalline packing. CB-2Se displayed a distinct (010) peak at $q_{xy} = 1.89 \text{ \AA}^{-1}$ in the in-plane direction, indicating that thermal annealing induced a transition from a face-on to an edge-on orientation, along with a pronounced reduction in the π - π

stacking distance from 3.59 to 3.32 \AA . Correspondingly, an intense (100) peak emerged at $q_z = 0.36 \text{ \AA}^{-1}$ in the out-of-plane direction, indicating an expanded lamellar spacing of 17.49 \AA . In addition, the coherence lengths of both the (100) and (010) peaks were estimated to be 39.6 nm and 18.5 nm , respectively, indicating larger crystalline domain sizes. These features facilitated charge transport in the OFET device and minimized the presence of grain boundaries, resulting in outstanding electron mobility and air stability. The major GIWAXS diffraction peaks of the thermally annealed CB-2Se thin film, particularly those at $q_z = 0.36 \text{ \AA}^{-1}$ and $q_{xy} = 1.89 \text{ \AA}^{-1}$, closely coincided with the corresponding peaks (0.35 \AA^{-1} and 1.86 \AA^{-1}) in the simulated single-crystal patterns, demonstrating that the CB-2Se film exhibited single-crystal-like characteristics. To simulate the molecular packing in the CB-2Se thin film further, I-Jui Hsu's team (National Taipei University of Technology) extracted the 1D scattering line-cut profiles in the q_{xy} and q_z directions from **Fig. 1(d)** and indexed them using typical powder X-ray diffraction programs, N-TREOR and DICVOL in the Expo2014 package. The simulated unit-cell packing model (**Fig. 2(a)**, see next page), along with the b-axis view (**Fig. 2(b)**), showed that CB-2Se molecules adopted an edge-on π - π stacking orientation along the b-axis on the substrate surface. Within the unit cell, two distinct dimeric arrangements emerged: an M-shaped core-to-terminal (CT) π - π stacking and an S-shaped CT-CT mode, both exhibiting tight π - π stacking distances— 3.38 and 3.35 \AA , respectively (**Fig. 2(c)**). Upon thermal annealing (**Fig. 2(d)**), the solution-processed CB-2Se film transformed from a kinetically trapped face-on configuration to a thermodynamically favored edge-on packing. This single-crystal-like arrangement, characterized by an edge-on orientation and an enlarged lateral coherence

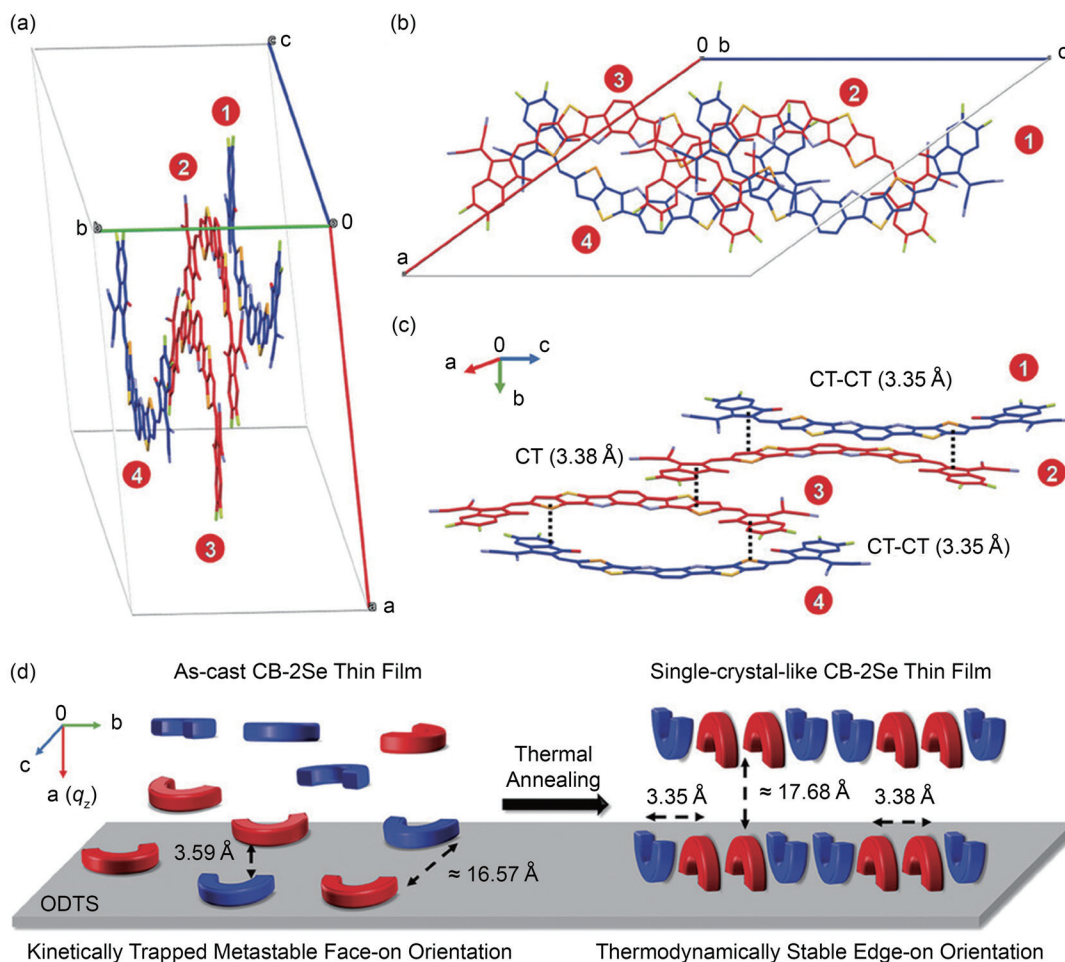


Fig. 2: (a) Simulated packing model in a unit cell of the thermally annealed CB-2Se thin film on the substrate (bc-face); (b) packing structure viewed along the b-axis; (c) side view showing the π - π distances of the dimeric CT and CT-CT modes; (d) illustration of the thermally induced transformation of the CB-2Se thin film from a face-on to an edge-on packing structure on the substrate. [Reproduced from Ref. 3]

length, effectively reduced grain boundaries and thereby lowered the trap density.

In summary, Se-substituted and symmetric NFA CB-2Se, with strong intermolecular interactions, enables the development of a single-crystal-like, solution-processed thin film that transitions from a kinetically trapped face-on π - π stacking orientation to a thermodynamically stable edge-on configuration upon thermal annealing. The CB-2Se-based OFET device achieved a remarkable electron mobility of $1.18 \text{ cm}^2 \text{ V}^{-1} \text{ s}^{-1}$ with exceptional n-type air stability, outperforming the corresponding A-D_NA_ND-A-type Y6-based materials by two orders of magnitude and representing the highest reported value for solution-processed n-type OFETs utilizing A-D-A-type small molecules. (Reported by Yen-Ju Cheng, National Yang Ming Chiao Tung University)

This report features the work of Yen-Ju Cheng and his collaborators published in Adv. Funct. Mater. 35, 2419176 (2025).

TPS 25A Coherent X-ray Scattering

- GIWAXS
- Materials Science, Organic Semiconductor

References

1. J. Yuan, Y. Zhang, L. Zhou, G. Zhang, H.-L. Yip, T.-K. Lau, X. Lu, C. Zhu, H. Peng, P. A. Johnson, M. Leclerc, Y. Cao, J. Ulanski, Y. Li, Y. Zou, *Joule* **3**, 1140 (2019).
2. Y.-J. Xue, Z.-Y. Lai, H.-C. Lu, J.-C. Hong, C.-L. Tsai, C.-L. Huang, K.-H. Huang, C.-F. Lu, Y.-Y. Lai, C.-S. Hsu, J.-M. Lin, J.-W. Chang, S.-Y. Chien, G.-H. Lee, U.-S. Jeng, Y.-J. Cheng, *J. Am. Chem. Soc.* **146**, 833 (2024).
3. K.-H. Huang, C.-C. Tseng, C.-L. Tsai, Y.-J. Xue, H.-C. Lu, C.-F. Lu, Y.-Y. Chang, C.-L. Huang, I. Hsu, Y.-Y. Lai, Y.-P. Zheng, B.-H. Jiang, C.-P. Chen, S.-Y. Chien, U. Jeng, C.-S. Hsu, Y.-J. Cheng, *Adv. Funct. Mater.* **35**, 2419176 (2025).